Vol. 37(1), pp. 47-71, June 2018
ISSN 1821-536X (print)
ISSN 2619-8789 (electronic)

Tanzania Journal of Engineering and Technology

Full Length Research Paper

Modelling of Flood Hazard and Susceptibility in Komatipoort, South Africa

Nomcebo Khumalo[1*], Aloyce W. Mayo[2] and Subira Munishi[2***]**

[1]35 Schatz Street, Nelsville, Nelspruit 1200, **South Africa**.
[*]Corresponding author E-mail: nomcebokhumalo@ymail.com
[2]Department of Water Resources Engineering
University of Dar es Salaam, P.O. Box 35131, Dar es Salaam, **Tanzania**.
[**]E-mail: aloyce.mayo@yahoo.com; [***]E-mail: evasubira@gmail.com

ABSTRACT

Komatipoort, a small town located at the confluence of Komati and Krokodil rivers, is constantly being hit by floods which affect the residents of this small town as well as the farmers settling along the rivers. This study aimed at mapping the flood hazard and susceptibility through the integration of GIS techniques and hydraulic modeling. Due to inconsistency in the length of streamflow data in the different gauging stations, a Hydrological modeling HBV model, was utilized for modelling runoff in order to extend flow records at station X2HO32 for Komati River. Calibration was conducted using observed data from 1982 to 1993, giving an efficiency value of 65% and validation was done using data from 1993 to 1999, giving an efficiency value of 53%. Flood frequencies were analyzed and flood quantiles were determined at different return periods. HEC-RAS was utilized to simulate the hydraulic parameters of Komati and Krokodil rivers to obtain flood hazard maps. GIS-based multi-criteria analysis techniques were incorporated for flood susceptibility mapping. Hydraulic analysis showed that the floods mostly affect the farms and settlements along the rivers and a small part of the central business district is affected. Flood susceptibility mapping showed that the area is generally highly susceptible to flooding because of a combination of anthropogenic and natural factors.

Key words: *Flood hazard; Komatipoort; Modelling; South Africa; Susceptibility.*

INTRODUCTION

Flood is described as a brief increase in the water level in a river to a maximum from which the level of water retreats at a slower pace (Kundzewicz, 2012). If water storage is limited because of elevated groundwater levels and the soil has high moisture levels, even low amounts of rainfall can cause a flood. Floods are arguably the most terrible of all natural disasters, with repercussions reverberating for years to come. They are the most recurrent natural disasters, and they rank as the third most destructive globally after rainstorms and earthquakes (Daniell, 2014). Floods are considered a serious societal and economical threat as they lead

to fatalities, loss of domestic resources, land properties, agricultural properties, settlements and roads (Swades and Surajit, 2012). Sayers *et al.* (2013) stated that streams always attract economical growth because they provide means for transporting goods, water supply domestic uses and farming, as well as electricity. Unfortunately, this places them at a high risk for floods, which cause massive fiscal and social losses, primarily as a consequence of spontaneous urbanization, unrestrained population growth and poor building control by authorities (Kundzewicz *et al.*, 2012).

Flood risk entails hazard and vulnerability. Hazards can never be modified; therefore reducing risk to a hazard can be best achieved through reduction of vulnerability of the population and environment to the hazard (Yashon *et al.*, 2014). Schanze *et al.* (2006) defined flood vulnerability as the extent of an area's inability to endure with the effects of floods. Kumpulainen (2006) concurs and further argued that vulnerability is the sum of damage potential and coping capacity. Flood susceptibility can be defined as the aspects at risk (human system, built and natural environment) within the systems, which influence the probability of being negatively affected during floods (Balica *et al.*, 2009).

According to the IFRC (2015) report, South Africa experiences local and wide-area floods, which tend to burden the country as a whole, as well as flash floods which affect local authorities. Flooding interrupts vital services such as communication systems, domestic water supply, transportation, electricity supply, wastewater management services, property damage and human fatalities. In accordance with Musungu *et al.* (2012), the occurrence of weather-related disasters has increased 2.4 times between 1970 and 2005, and they are projected to escalate even further. Studies forecast increased rainfall intensity episodes in South Africa, which is the main determinant for floods, but other contributing factors include land use, type of soil, topography and catchment area. Musungu *et al.* (2012) further stated that the climate change is likely to increase flood risk due to elevated sea levels as well as more intense rains which will lead to high stream flows. Floods have become more prevalent in South Africa, including Komatipoort area, which is particularly susceptible to floods. According to the Lowaevelder local newspaper dated 05th March 2014, raging floods swept the Komatipoort area, destroying life and property. Roads had to be closed off and people who could not leave via the usual routes were airlifted by helicopters. Bridges were washed away, vehicles were swept away, houses were flooded, and water treatment plants were destroyed (Khumalo, 2016). Divers worked around the clock rescuing people and retrieving bodies of people who had drowned. This is not an isolated case, as News24 had previously reported similarly destructive floods in January 2012 and January 2013 (Khumalo, 2016). The main objective of this study is to estimate flood quantiles for different return periods and to evaluate and map flood hazard and susceptibility in Komatipoort area.

METHODS AND MATERIALS

Description of the Study Area

Komatipoort is a small town located at the convergence of the Krokodil and Komati Rivers under the jurisdiction of Nkomazi Municipality in the Ehlanzeni region, Mpumalanga province in the Republic of South Africa (Figure 1). The town is 8 km from the Crocodile Bridge Gate into the Kruger National Park, a mere 5 km from the Mozambique border and 65 km from the Swaziland border. It is a diminutive, sleepy town within the Lowveld with an area of 11.71 km^2 and a population of approximately 20,508, according to the

2011 National Census. It is one of the hottest towns in South Africa, with temperatures that can rise to as high as 48°C in the peak of summer, and winter temperatures of 24 °C. It lies at coordinates 25°26′S and 31°57′E. The elevation of Komatipoort ranges from 29 to 377 m.a.s.l. and the slope ranges from 0 to 57%. The land uses in Komatipoort are urban / built-up, industries, indigenous forest, thicket, bush land, woodlands, shrub land, agricultural land (sugarcane, orchards), barren land, water bodies and wetlands. Figure 2 shows the land use of Komatipoort.

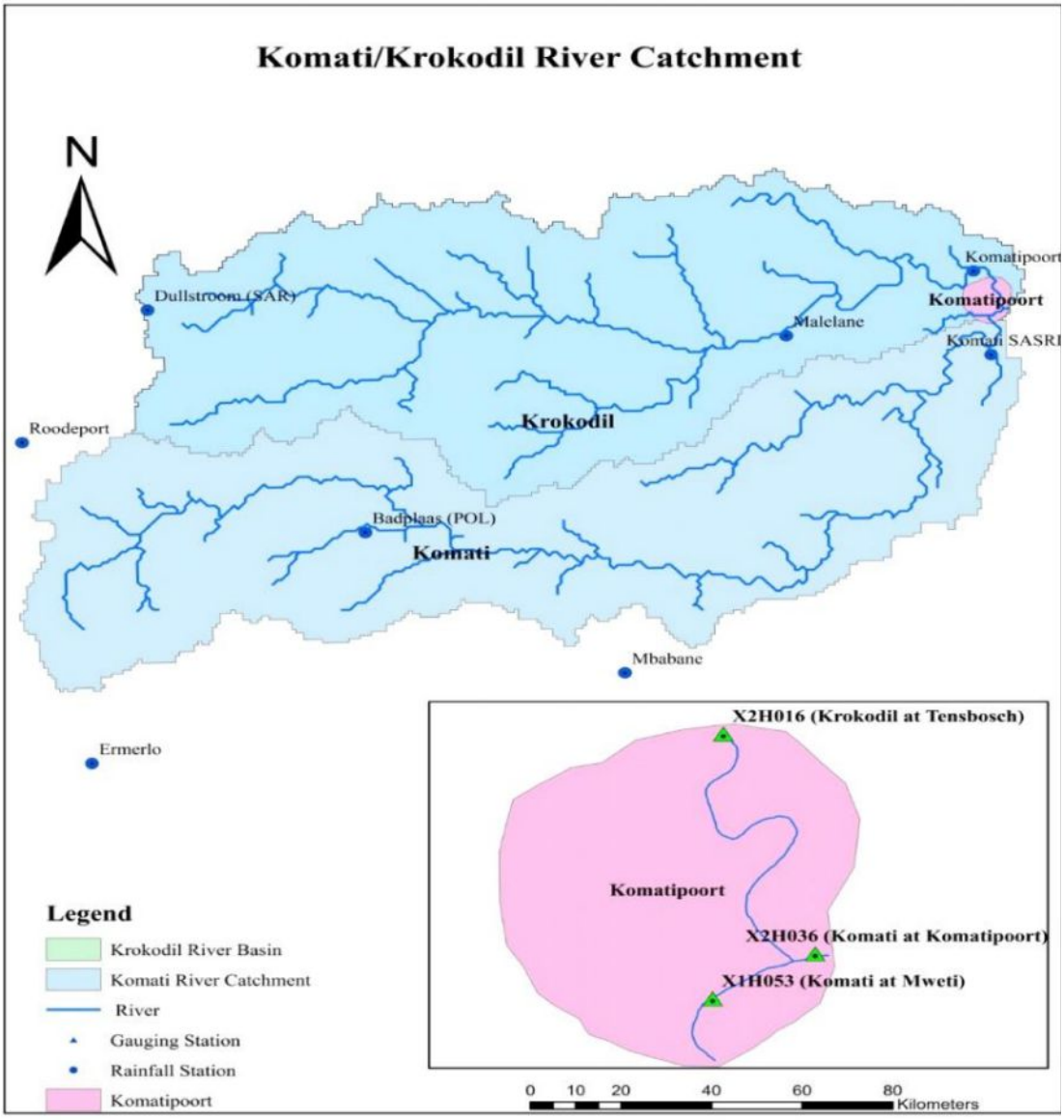

Figure 1: Komatipoort within Komati/Krokodil Catchment

Hydrological and Hydraulic Analyses

In an endeavor to meet the specific objectives of this research, hydrological and hydraulic analyses were carried out to obtain a flood inundation map, and further highlights the data requirement at each step of analysis (Figure 2). In hydrological

analysis, HBV (Hydrologiska Byråns Vattenbalansavdelning) model was utilized to obtain an reconstruct streamflow data for Komati catchment, using observed, historical data as an input. Data for Komati catchment flow area had to be extended because it was shorter than the Krokodil Catchment flow data.

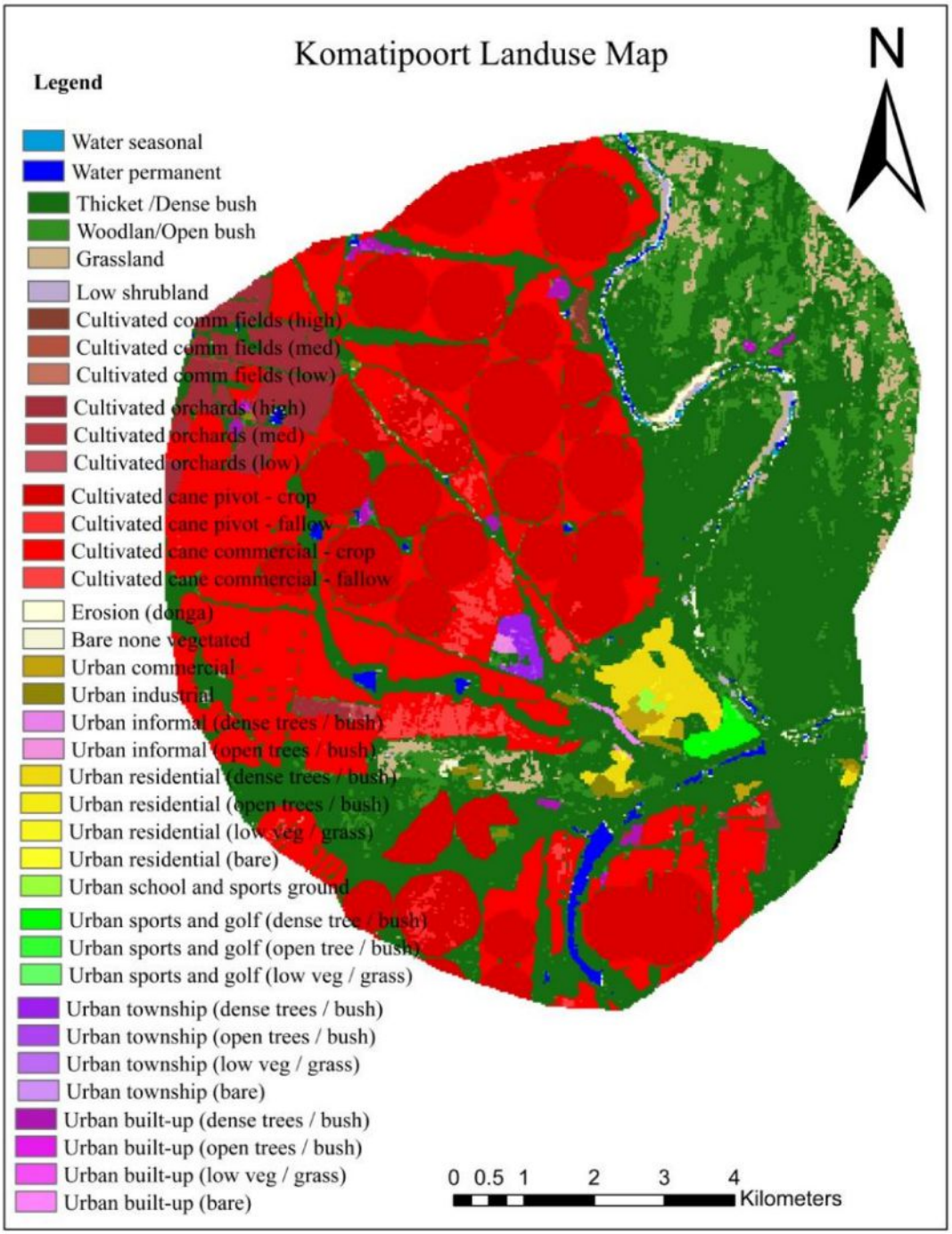

Figure 2: Komatipoort Land use

Stream discharge peaks were selected from the flow data and used in EasyFit, a frequency analysis software, to obtain flood quantiles for different return periods. In hydraulic analysis, the flood quantiles were utilized in HEC Geo-RAS

(Hydrological Engineering Centre – Geospatial River Analysis System) to obtain river channel geometry and cross-sections, which were utilized as input in HEC-RAS (Hydrological Engineering Centre River Analysis System) to obtain the water levels and stream velocity, which in turn was used in Geo-RAS to obtain the flood inundation map, as illustrated in Figure 3.

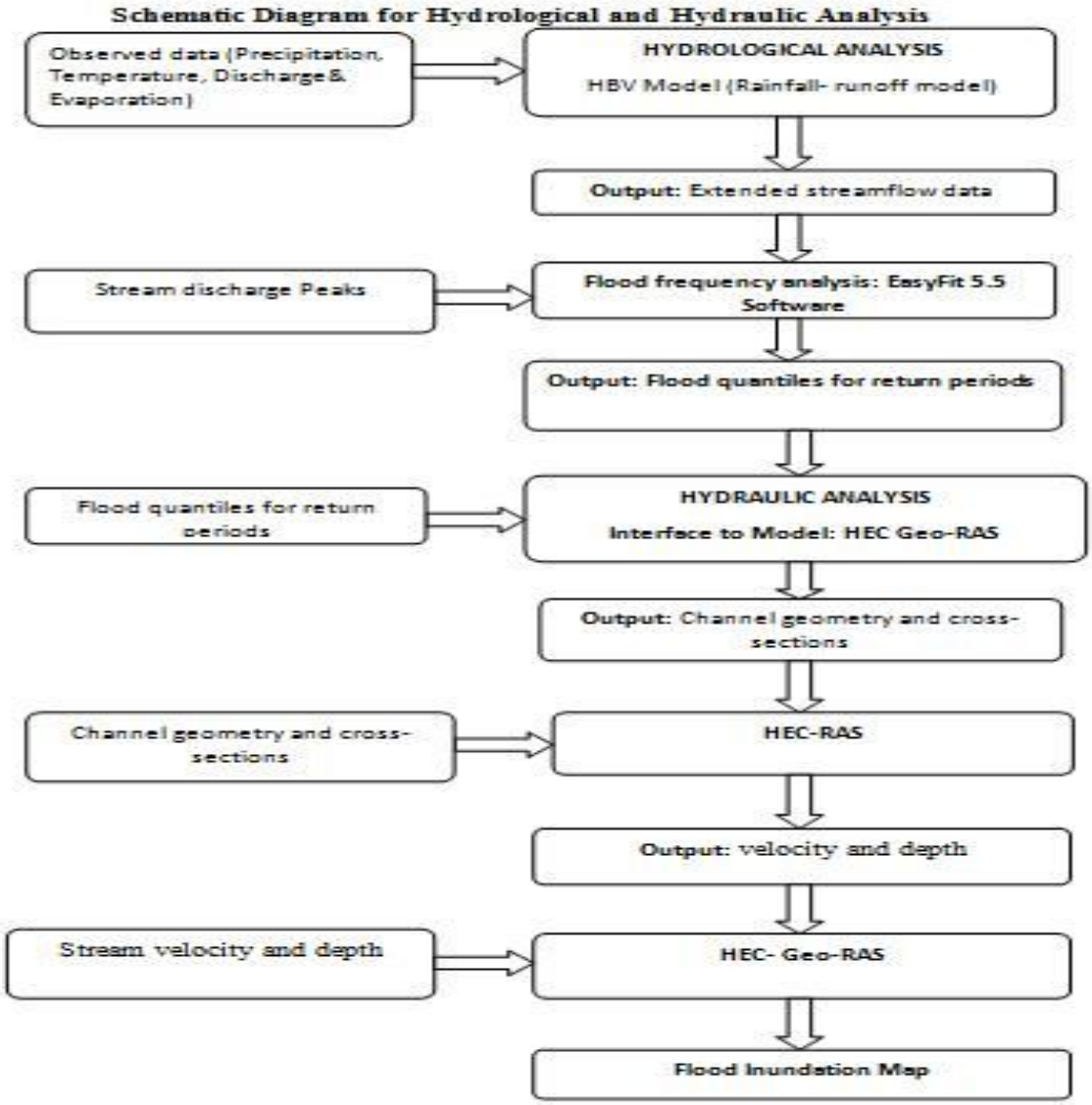

Figure 3: Hydrological and hydraulic analysis

Hydrological modeling of streamflow

Due to inconsistency in the length of streamflow data for Komatipoort in the 3 gauging stations, a rainfall-runoff model, HBV, was utilized for the reconstruction of runoff data from the rainfall in order to extend (backward) the data for Komati at Mweti (Upstream) station from 1982 to 1968. The input data required by HBV model in order to simulate streamflow consists of daily values of precipitation, temperature, discharge and total evaporation. The Komati River (upstream) catchment area has 8 rainfall stations; Roodepoort, Ermelo, Dullstroom, Badplaas, Mbabane, Komati SASRI, Komatipoort and Malelane. The Thiessen polygon method was used to establish the weight of each station towards the

catchment rainfall, and thus obtaining the catchment precipitation. The daily rainfall and temperature data for the rainfall stations were acquired from the South African Sugar Cane Research Institute (SASRI). The catchment has 3 gauging stations with daily streamflow data. This data was obtained from the Department of Water and Sanitation/hydrology, Government of South Africa. Hargreave's method was used to determine total evaporation, as illustrated in equation (1).

$$ET_o = a + b\frac{0.0023R_a}{\lambda}\left(\frac{T_{\max}+T_{\min}}{2}+17.8\right)\sqrt{T_{\max}-T_{\min}} \quad \text{..... (1)}$$

Where; T_{max} = maximum daily air temperature (°C); T_{min} = minimum daily air temperature (°C); R_a = extra-terrestrial solar radiation (MJ m^2/day); a = 0 (mm/day): a calibrated co-efficient determined on a monthly/yearly basis by regression analysis or visual fitting; b = 1 (mm/day): a calibrated co-efficient determined on a monthly/yearly basis by regression analysis or visual fitting.

Model calibration, verification and application

The model was calibrated using Gap optimization. However for peak discharge, difficulties were experienced in simulation of peak discharge and its timing and therefore, manual calibration was used to overrun the auto-calibration. In order to carryout historical streamflow data reconstruction for the period from 1968 to 1981, the primary data from 1982 to 1993 was used for model calibration, while data from 1993 to 1999 were used for model validation. This therefore provided 13 years of reconstructed discharge data *i.e.* from 1968 to 1981.

Estimation of flood quantiles for different return periods

Flood frequency was carried out using statistical analysis of annual maximum flood series. This was possible because long records of streamflow data were available. Flood frequency analysis was done with the help of EasyFit software that used the annual maximum flood series as input in order to establish the most appropriate frequency distribution that best fits the annual maxima data. The goodness-of-fit tests of Kolmogorov-Smirnov, Anderson Darling and Chi-Squared were carried out using the following selection criteria:

- Lowest overall score 2 parameter test, in which the probability distributions that were getting the lowest combined overall scores of Kolmogorov-Smirnov and Anderson Darling parameters were selected as possible candidates.
- Lowest overall score 3 parameter test, in which the probability distributions that were getting the lowest combined overall scores of Kolmogorov-Smirnov, Anderson Darling and Chi-Squared parameters were selected as possible candidates.
- Common in hydrology, whereby only probability distributions which are familiar in hydrology were selected as possible candidates.
- The Q-Q plot was used to visualize how each probability distribution performs when the peaks were plotted. The distributions that best fitted the data series at different discharge ranges were selected and recorded. Each distribution was used to estimate the flood quantiles for different return periods, using the probability distribution parameters and cumulative frequency as input according to equation (2).

$$F(x) = P = 1 - \frac{1}{T} \quad \text{..... (2)}$$

Where T is return period. The estimate quantile ($Q_{(P)}$) is equal to the quantile for specific return period ($Q_{(T)}$) for each distribution. The final flood quantiles for each period were then selected based on

the selected distributions for each flood range.

Flood hazard mapping in Komatipoort

A 30 x 30 DEM of Komatipoort and Google earth map was used for flood zoning. The Google earth map was geo-referenced in Arc GIS. The application of Geographical Information System (GIS) in flood risk mapping can range from storing and organizing hydrological data to producing flood inundation maps in order to support flood risk management (Bishaw, 2012). Geometric key data for HEC-RAS model was formed using HEC-GeoRAS software, which is an extension of ArcGIS computer package for spatial analysis. In HEC-GeoRAS, geometric layers such as the river center line, flow paths, bank lines, cross sections, and bridges were generated by digitizing, using the Google earth map as reference. The essential attributes were allocated to each of these layers. The data was then imported to HEC-RAS for further analysis (Sredojevic and Simonovic, 2009).

To establish flood levels, a statistical analysis of the discharge data was executed in order to derive the probability of occurrence of floods. The geometric data was imported from HEC-geoRAS into HEC-RAS. Manning's "n" values were entered for each cross section, using the land use map as reference. The steady flow data and discharge with different return periods was also added, and the boundary conditions were determined. Data on bridges, derived from the existing models and drawings were incorporated with the rest of the data and a normal depth was calculated based on the slope. After entering all of the required data, the simulation was carried out and the water surface profiles were extracted. The HEC-RAS model results were then added into HEC-geoRAS, flood zones were extracted. HEC-GeoRAS was used to extract water surface profile data from HEC-RAS and was incorporate it into a floodplain map in GIS, thus displaying the inundation for different return periods.

Determination of flood susceptibility in Komatipoort

Susceptibility indicators determine how perceptively an aspect at risk performs when it is exposed to hazard. Flood susceptibility is determined by anthropogenic factors (land use and road density), hydrological factors (drainage density), geomorphological factors (slope and elevation) as well as meteorological factors (rainfall), as illustrated in Figure 4. The flood susceptibility map of Komatipoort was developed using GIS evaluation techniques. GIS layers were prepared for land use, drainage density, slope, road density, rainfall, and elevation. Elevation and slope were derived from the DEM. Road density and drainage density were calculated in GIS using the drainage map and road map, respectively. These contributing maps were all converted to raster and reclassified, as illustrated in Figure 5. The contributing properties of each factor were ranked, and weights were assigned to each of the factors as an indication of the level of significance towards flood risk (Table 1).

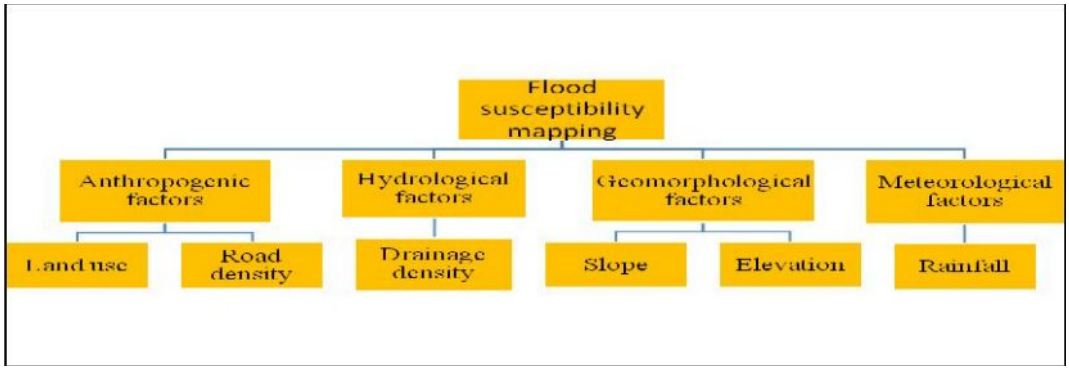

Figure 4: Flood Susceptibility Factors

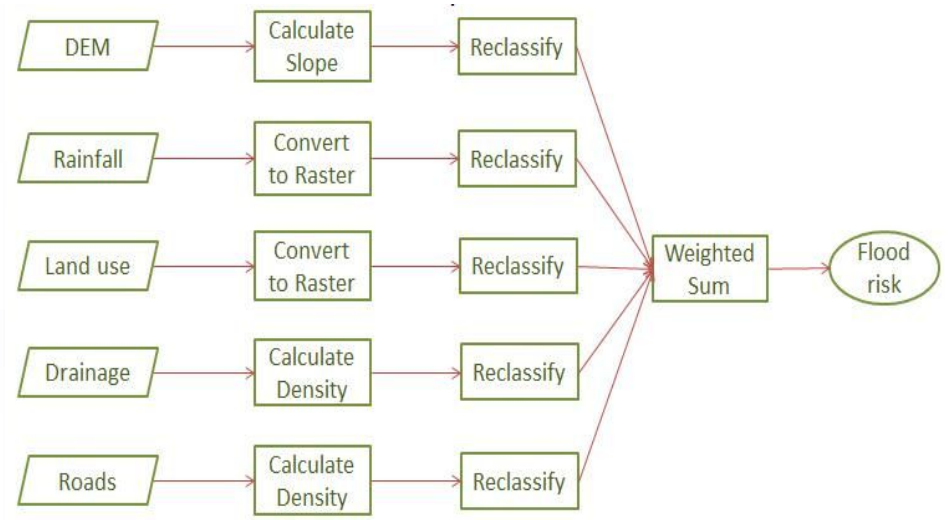

Figure 5: Schematic diagram for flood Susceptibility Mapping (Malczewski, 1999)

Flood susceptibility was determined based on a number of indicators such as rainfall, land use, elevation slope, drainage density and road density. Heavy rainfall is one of the major causes of floods, hence it carries the most weight in flood susceptibility analysis. In Arc GIS, extreme rainfall values for all the rainfall stations which fall within the catchment of the study area were plotted and interpolated using the Krigging method in order to obtain a rainfall map. The rainfall values were then reclassified in accordance with the flood susceptibility ranking scheme of 1 to 5, with 1 denoting very low rainfall, thus representing very low susceptibility to floods and 5 denoting very high rainfall, therefore representing very high susceptibility to floods.

The land use map for Komatipoort was also reclassified like the rainfall map for determination of flood Susceptibility based on land use. The value 1 denotes limited land use change, meaning the area is mostly covered in forests, thus facing very low susceptibility to floods, 2 represents rangeland which poses low susceptibility, 3 is agricultural land which is moderately susceptible, 4 is barren land with high flood susceptibility and the value 5 denotes urban built-up, wetlands and water bodies dominance in the area, therefore representing very high susceptibility to floods.

Table 1: Flood Susceptibility Criteria (Source: Malczewski, 1999).

Factors	Weight	Classification scheme	Ranking scheme	Ranked Values
Rainfall (mm)	3	0 – 150	Very Low	1
		151 – 200	Low	2
		201 – 250	Moderate	3
		251 – 300	High	4
		301 – 350	Very High	5
Elevation (m)	2	300.1 – 450	Very low	1
		150.1 – 300	Low	2
		75.1- 150	Moderate	3
		25.1 – 75	High	4
		0 – 25	Very High	5
Slope (degrees)	2	29 – 35	Very low	1
		22 – 28	Low	2
		15 – 21	Moderate	3
		8 – 14	High	4
		0 – 7	Very High	5
Drainage Density (5000m pixel)	2	0 – 7000	Very low	1
		7001 – 14000	Low	2
		14001 – 21000	Moderate	3
		21001 – 28000	High	4
		28001 – 35000	Very High	5
Road Density (5000m pixel)	1	0 – 15000	Very low	1
		15001 – 30000	Low	2
		30001 – 50000	Moderate	3
		50001 – 60000	High	4
		60001 – 70000	Very High	5
Land Use (related to water absorption and drainage capacities)	1	Forest	Very Low	1
		Rangeland	Low	2
		Agricultural land	Moderate	3
		Barren land	High	4
		Urban, Wetlands, Water bodies	Very High	5

The elevation map of Komatipoort was derived from the DEM using in GIS and also reclassified for determination of flood Susceptibility based on the elevation. The value 1 denotes very high elevation, thus representing very low susceptibility to floods and the value 5 denotes very low elevation, therefore representing high susceptibility to floods. With elevation, the higher the elevation value, the lower the flood susceptibility, and the lower the value, the higher the susceptibility.

Flood susceptibility based on slope involved derivation of the slope map of Komatipoort from the DEM through Spatial Analyst Tools in Arc GIS and reclassified, then ranked with the value 1 denoting very high slope, thus representing very low susceptibility to floods and the value 5 denoting very low slope, therefore representing high susceptibility to floods. With slope, the higher the slope value, the lower the flood susceptibility, and the lower the value, the higher the susceptibility.

Flood susceptibility based on the drainage density required derivation of drainage density map of Komatipoort from stream networks through Focal Statistics in Arc GIS. The drainage density map was further reclassified in Arc GIS, with 1 denoting very low drainage density, thus representing very low susceptibility to floods and 5 denoting very high drainage density, therefore representing very high susceptibility to floods.

The road density map of Komatipoort was derived from roads map through Focal Statistics in Arc GIS in order to determine flood susceptibility based on road density. The road density map was further reclassified in Arc GIS, with 1 denoting very low road density, thus representing very low susceptibility to floods and 5 denoting very high road density, therefore representing very high susceptibility to floods. The flood susceptibility map for all factors was the weighted sum map (Flood susceptibility), which was developed in Arc GIS using the following map algebra expression:

Weighted Sum = (Rainfall Value x 3) + (Drainage Value x 2) + (Slope Value x 2) + (Elevation x 2) + (Road Density Value) + (Land Cover Value).

All 6 input maps were added in Arc GIS, and the final map was obtained through the use of raster calculator in Map algebra under Spatial Analyst Tools, using the weighted sum algebra expression. Just like the input maps, the flood susceptibility map was also reclassified in Arc GIS using the ranking scheme of 1 to 5, with 1 denoting very low flood susceptibility to floods, 2 denoting low flood susceptibility, 3 denoting moderate flood susceptibility, 4 denoting high flood susceptibility and 5 denoting very high susceptibility to floods. For ease of use, the traffic light approach was used, i.e. red for high susceptibility and green for low susceptibility.

RESULTS AND DISCUSSIONS

Extension of streamflow data for Komati catchment

Inconsistency in the length of flow data in the different gauging stations of Komatipoort called for extension of the said data. Flow data for Komati Catchment was extended because it was shorter than Krokodil Catchment flow data. This was achieved through the utilization of HBV, a rainfall-runoff model which simulates runoff from observed precipitation data and also has the ability to extend the data for previous, unrecorded years. The results show that Badplaas rainfall station has the highest rainfall contribution towards the catchment at 35%, followed by Malelane Rainfall station at a 24% contribution, then Roodepoort at 12%, Ermelo at 7%, Komatipoort at 3%, and Mbabane at 2%, while Dullstroom and Komati SASRI stations show no contribution towards the catchment. This is illustrated in Figure 6. Table 2 also shows that most of the rainfall stations have missing data. Roodepoort rainfall station has 2.42% missing data, Ermelo has 0.85%, Dullstroom has 8.5%, Badplaas has 1.84%, Mbabane has 0.92%, Komati SASRI has 0.11%, Malelane has 0.98% and Komatipoort has no missing data.

Table 2: Komati River Catchment Rainfall Stations Inventory

No.	Rainfall Station	Location (Lat, Long)	Data range	% missing data	Contribution weight towards catchment area
1.	Roodepoort	-25.73, 29.82	1905 - 2000	2.42	0.12
2.	Ermelo	-26.52, 29.95	1942 - 1991	0.85	0.07
3.	Dullstroom	-25.42, 30.10	1906 - 1993	8.5	0
4.	Badplaas	-25.97, 30.52	1911- 2000	1.84	0.35
5.	Mbabane	-26.32, 31.13	1903 - 1994	0.92	0.2
6.	Komati SASRI	-25.55, 31.95	2001 - 2016	0.11	0
7.	Komatipoort	-25.35, 31.91	1965 - 1995	0	0.02
8.	Malelane	-25.50, 31.50	1938 - 2000	0.98	0.24

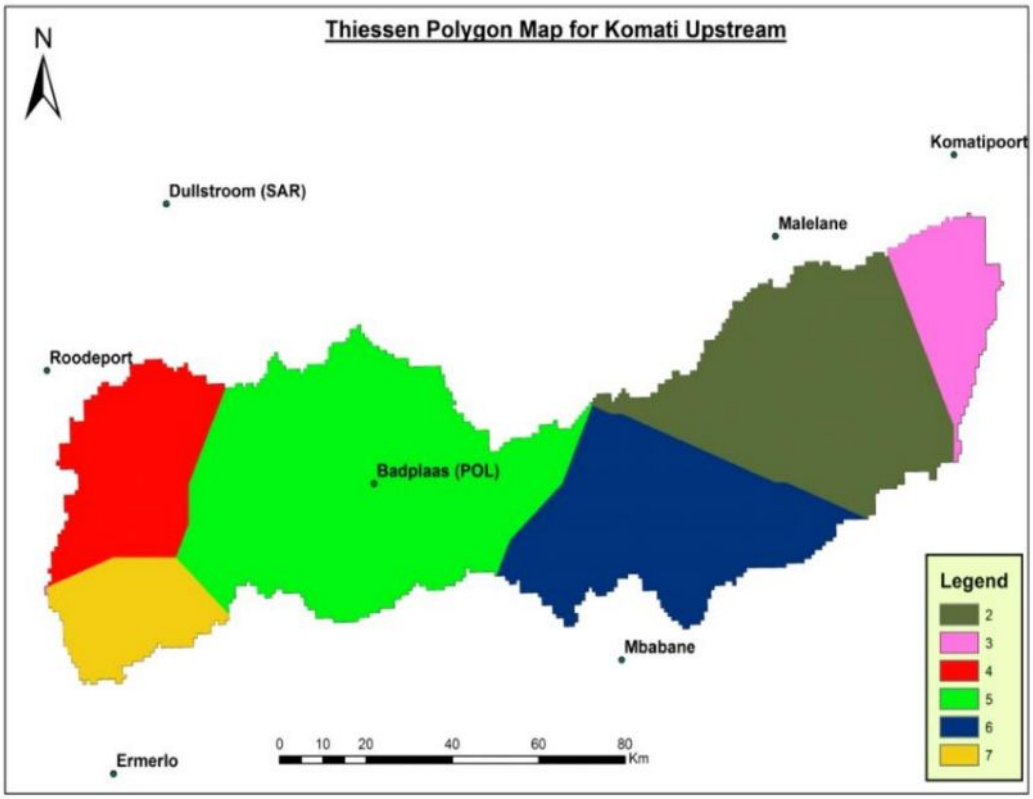

Figure 6: Thiessen Polygon Map for Komati River Catchment

Table 3 shows a good streamflow records with minimal data missing.. Gauging stations X1HO53, X2HO16 and X2HO36 had 9.18%, 9.0% and 9.2% missing data, respectively. Streamflow data from Station X2HO36 (Komati at Mweti) was used in HBV model because it is the data that required extension in order to match data from station X2HO16.

Table 3: Komati/Krokodil River Catchment Streamflow Inventory

No.	Gauging Station	Location (Lat, Long)	Data range	% Missing Data
1.	X1HO53	-25.451, 31.95	2006 - 2016	9.18
2.	X2HO16	-25.36, 31.96	1960 - 2016	9.0
3.	X2HO36	-25.44, 31.98	1982 - 2016	9.2

HBV Model calibration and validation

Model calibration was conducted using data for the period of 1st October 1982 to 30th September 1993, and a model efficiency of 65% was obtained through Gap optimization. The parameters were adjusted manually for peaks that were not fitting well since auto-calibration was failing to capture all the peaks. Historical data was obtained by using the wettest years (1983/84 and 1984/85) as input for the first set. The rest of the peaks were captured by conducting annual calibration (Figure 7). Table 4 and 5 show the parameters that were optimized in HBV model during calibration exercise in an effort to simulate the extreme floods and small and moderate floods, respectively.

Table 4: Optimized HBV Parameters used to capture extreme floods

Parameter	Description	Range	Optimized Value
FC	Maximum soil moisture storage	50 - 500	142.56
LP	Soil moisture value above which AET reaches	0.3 - 1	0.90
BETA	Parameter that determines the relative contribution of runoff from rain and snowmelt.	1.0 – 4.0	4.17
PERC	Threshold parameter	0.5 – 2.0	4.42
UZL	Threshold parameter	10 - 100	13.0
K0	Storage coefficient 0	0.1 – 1.0	0.712
K1	Storage coefficient 1	0.01 – 1.0	0.241
K2	Storage coefficient 2	0.001 – 1.0	0.073
MAXBAS	Change of precipitation with elevation	1 – 2.5	0.073

Model validation was carried out to check the ability of the model to perform with a definite eminence of intended purpose. Model validation was carried out using data for the period of 1st October 1993 to 30th September 1999, with a model efficiency of 53%. The results in Figure 8 show a good relationship between simulated and observed flows, although there is a markedly high difference between observed and simulated flows at extremely high flows between the years 1983 and 1984. Since acceptable model efficiencies were obtained for calibration and validation (65% and 53%, respectively), the model was then run in order to extend the data from 1982 to 1968, thus giving 13 years of extended stream flow data, as shown in Figure 9.

Table 5: Optimized HBV Parameters used to capture small to moderate floods

Parameter	Description	Range	Value
FC	Maximum soil moisture storage	50 - 500	226.65
LP	Soil moisture value above which AET reaches	0.3 - 1	0.94
BETA	Parameter that determines the relative contribution of runoff from rain and snowmelt	1.0 – 4.0	2.62
PERC	Threshold parameter	0.5 – 2.0	2
UZL	Threshold parameter	10 - 100	99.57
K0	Storage coefficient 0	0.1 – 1.0	0.8
K1	Storage coefficient 1	0.01 – 1.0	0.7
K2	Storage coefficient 2	0.001 – 1.0	0.17
MAXBAS	Change of precipitation with elevation	1 – 2.5	5.28

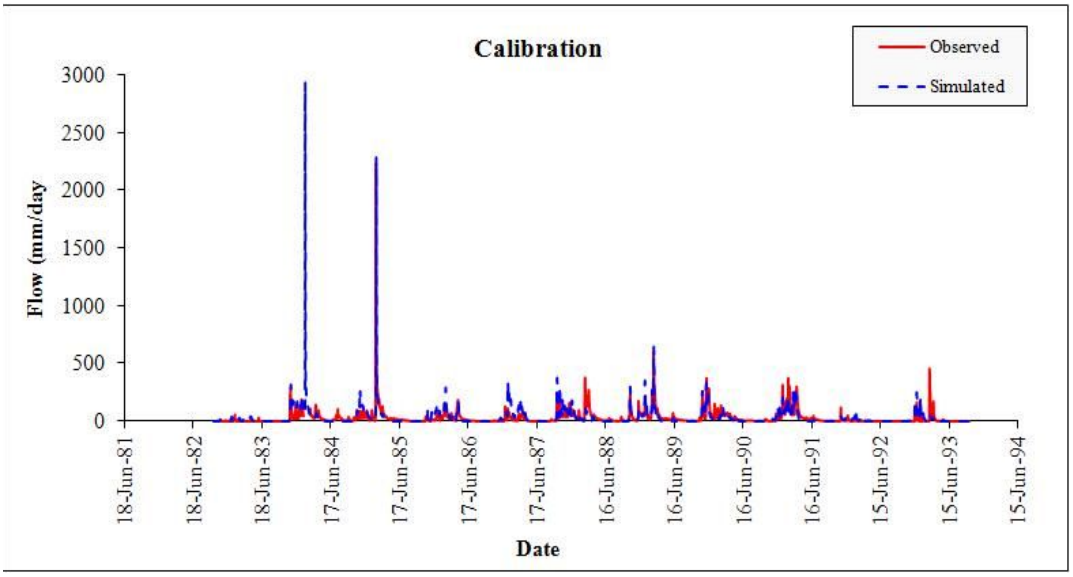

Figure 7: Model Calibration at Komati River Catchment

Estimation of flood quantiles for different return periods

Flood frequency analysis

Since long records of flow data are available, a flood frequency analysis of observed data was conducted and EasyFit software was utilized, using annual flow peaks as input in order to establish the type of probability distribution that best fit these flow peaks. The goodness-of-fit tests (Kolmogorov-Smirnov, Anderson Darling and Chi-Squared) were conducted using the 2 parameter test and 3 parameter test.

In determining the best probability distribution for Krokodil River using the 2 parameter test, Frechet (3P) distribution ranked the best at position 4, but in the 3 Parameter test, Log Logistic (3P) ranked the highest at 10. However, in the overall test, Log Logistic (3P) ranked the highest (Table 6). In determining the best probability distribution for Komati River using the 2 parameter test, Gumbel Max distribution ranked the best at position 3, but in the 3 Parameter test, Weibull ranked the highest at 25 and in the overall test, Weibull ranked the highest (Table 7).

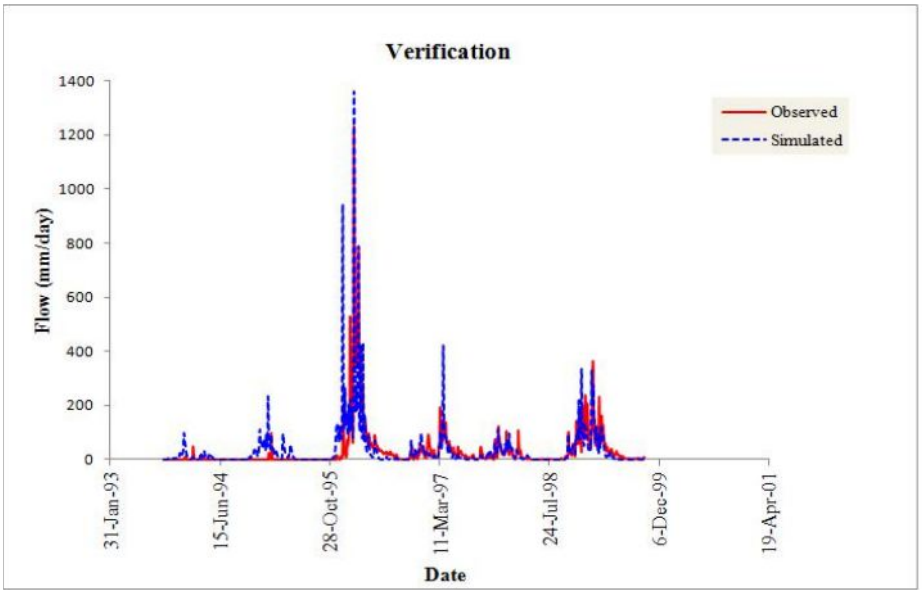

Figure 8: Model Validation at Komati River Catchment

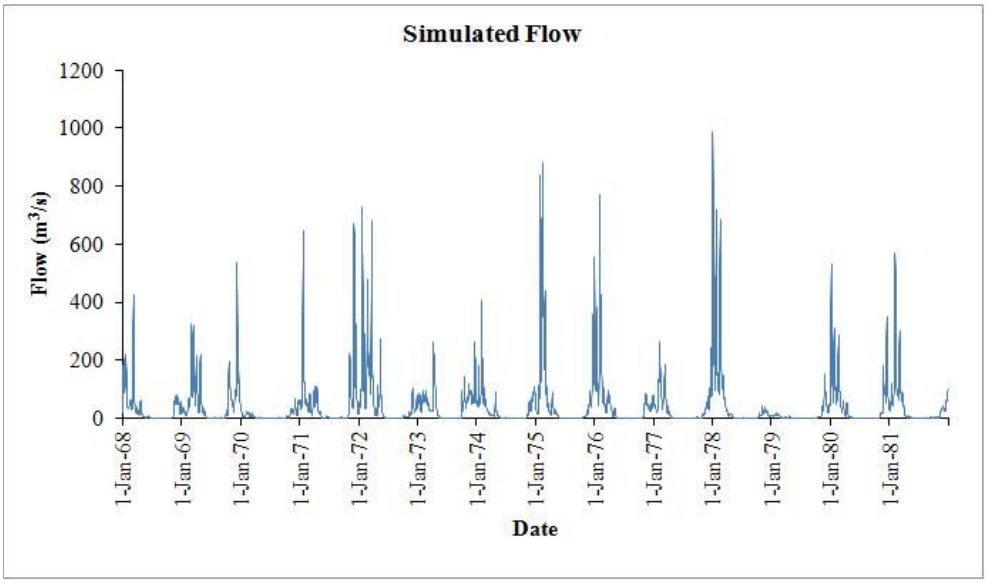

Figure 9: Flow extension by HBV Model at Komati River Catchment

Table 6: Parameter test for Krokodil

Distribution	Kolmogorov -Smirnov	Anderson Darling	Chi-Squared	2P Test	3 P Test	Overall Rank
Log-Gamma	9	9	1	18	19	5
Log-Logistic(3P)	1	6	3	7	10	1
Pearson (3P)	5	4	6	9	15	4
Dagum	4	3	7	7	14	3
Frechet (3P)	2	2	8	4	12	2

Table 7: Parameter test for Komati

Distribution	Kolmogorov -Smirnov	Anderson Darling	Chi-Squared	2P test	3P test	Overall Rank
Gumbel Max	1	2	23	3	26	2
Gen. Extreme Value	9	3	34	12	46	5
Dagum	8	12	7	20	27	3
Burr	4	14	14	18	32	4
Weibull	2	10	13	12	25	1

After obtaining the results from the first 2 tests (2 parameter and 3 parameter tests), only the probability distributions which are familiar in hydrology were selected. The uncommon ones such as Burr and Dagum were disqualified. The Q-Q plot was also used to visualize the performance of each probability distribution when the data series was plotted. The distributions that best fitted the data series at different discharge ranges were selected and recorded. Figure 10 illustrates Gamma Q-Q Plot for Krokodil River. Table 8 shows the best probability distributions for Krokodil River flow data. Log Logistic (3P) gave a good fit at discharges that are less or equal to 400 m^3/s, Reciprocal was good for discharges at the range of 400 to 500 m^3/s, and Gamma was suitable for discharges ranging above 500 to 1200 m^3/s.

Table 8: Best distribution for Krokodil River

Best Distribution (Krokodil River)	Parameters			Discharge range (m^3/s)
	α	β	γ	
Log-Logistic (3P)	1.37	214.31	17.22	≤ 400
Reciprocal	43.1	2927	-	400 - 500
Gamma	1.81	201.37	0	500 - 1200

Table 9 demonstrates the best probability distributions for Komati River flow data. General Pareto gives a suitable fit at discharges that are less or equal to 200 m^3/s, Uniform is good for discharges at the range of 200 to 400 m^3/s, Pareto 2 performs well at the range of 400 to 500 m^3/s, Gamma is suitable for discharges ranging above 500 to 1250 m^3/s, Log Logistic (3P) performs well at the range of 1250 - 2250 m^3/s and Reciprocal is suitable for ranges exceeding 2250 m^3/s. These probability distributions are selected based on the Q-Q plot of each distribution to visualize its performance when the data series is plotted.

Table 9: Best distribution for Komati River Upstream

Best Distribution (Komati River upstream)	Parameters			Discharge range (m^3/s)
General Pareto	k – -0.334	450.4	μ – 19.0	≤ 200
Uniform	α – -103.7	β – 816.5		200 – 400
Pareto 2	α –-109.0	β – 16.5		400 - 500
Gamma	α = 1.8	β = 198.0	γ = 0	500 - 1250
Log Logistic (3P)	α = 1.7	β = 284.6	γ = 17.38	1250 - 2250
Reciprocal	α = 43.1	β = 2927	-	> 2250

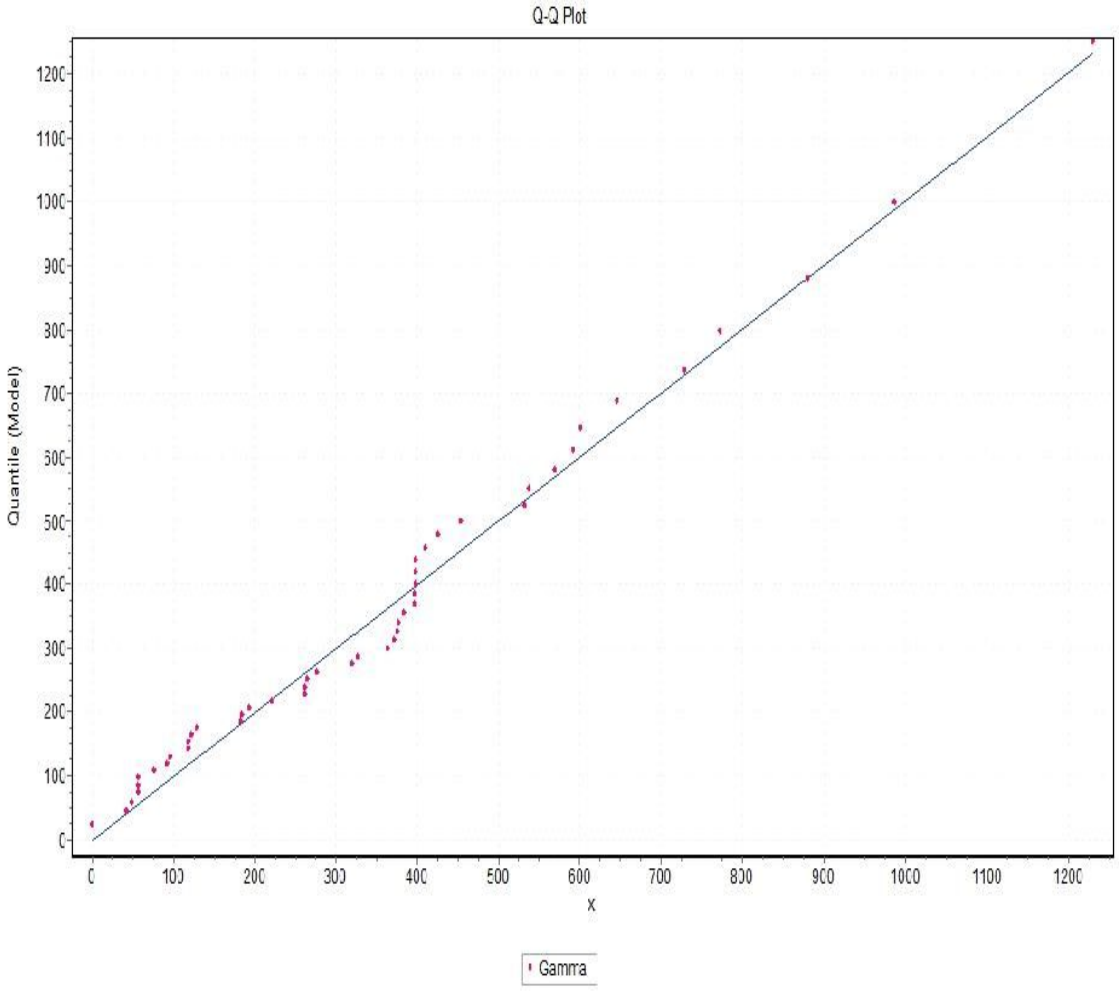

Figure 10: Gamma QQ Plot for Krokodil River

Flood Quantiles for Different Return Periods

Table 10 shows the flood quantiles for the different return periods for all 3 probability distributions. Each selected probability distribution was used to estimate flood quantiles for different return periods in EasyFit software by using the probability distribution parameters and cumulative frequency as input. The cumulative frequency was obtained using equation (2). These 3 sets of flood quantiles were compared with the already established ranges of the probability distributions in order to obtain the final flood quantiles. The final flood quantiles for Krokodil River are 142 m^3/s for a 2-year return period, 336 m^3/s for a 5-year return period, 738 m^3/s for a 10-year return period, 929 m^3/s for a 20-year return period, 972 m^3/s for a 25-year return period, 1066 m^3/s for a 50-year return period, 1116 m^3/s for a 100-year return period, 1158 m^3/s for a 500-year return period, and 1163 m^3/s for a 1000-year return period.

Table 10: Flood quantiles for Krokodil River

T	F(x)	Q_T Krokodil (m^3/s)			
		Gamma	Log Logistic (3P)	Reciprocal	Final Flood quantiles
2	0.5	159	142.37	193.2	142.4
5	0.8	372.1	336.24	479.9	336.2
10	0.9	560.2	671.3	737.8	737.8
20	0.95	831.5	897.1	928.6	928.6
25	0.96	1024.2	1010.1	972.4	972.4
50	0.98	1057.9	1157.3	1066.1	1066.1
100	0.99	1278.5	1221.4	1116.2	1116.2
500	0.998	1297.2	1257.3	1158.1	1158.1
1000	0.999	1354.8	1330.9	1163.4	1163.4

These results indicate that, a flood with a discharge of 142 m^3/s is likely to recur in the study area every 2 years, a flood with a discharge of 336 m^3/s is likely to recur every 5 years, etc. According to this analysis, a flood of 1066 m^3/s is likely to occur every 50 years, which was found to be accurate considering that in the streamflow data for Krokodil River observed over 55 years, the maximum flow is 1169 m^3/s, and the second highest flow is 1022 m^3/s. Moreover, EasyFit software has proven to be a reliable tool for flood frequency analysis.

Table 11 shows the flood quantiles for the different return periods for all 3 probability distributions. These 6 sets of flood quantiles were compared with the ranges of the probability distributions in order to obtain the final flood quantiles. The final flood quantiles for Komati River are 356 m^3/s for a 2-year return period, 540 m^3/s for a 5-year return period, 711 m^3/s for a 10-year return period, 874 m^3/s for a 20-year return period, 926 m^3/s for a 25-year return period, 1048 m^3/s for a 50-year return period, 1240 m^3/s for a 100-year return period, 2903 m^3/s for a 500-year return period, and 2905 m^3/s for a 1000-year return period. This analysis is acceptable, considering that in the streamflow data for Komati River of 47 years, the maximum flow recorded is 2927 m^3/s, and the second highest flow is 2210 m^3/s.

Flood Hazard Mapping in Komatipoort

Figure 11(A) shows the geometric layers that were generated in HEC Geo-RAS and imported to HEC RAS for further analysis for Komati and Krokodil rivers. This geometric data includes the river centre line, flow paths, bank lines, reaches, cross-sections, and bridges. The upper reach is Komati River upstream, the lower reach is Komati River downstream and Krokodil River is the tributary, as developed in HEC Geo-RAS. Figure 11(B) is a cross-section of Komati River showing the flood depth at different return periods. At this point, the flood depth is 14 m. Figure 11(B) also shows a high elevation, which suggests the presence of a hill or a mountain.

Table 11: Flood quantiles for Komati River

T	F(x)	Q_T Komati (m^3/s)						
		General Pareto	Uniform	Pareto 2	Gamma	Log Logistic (3P)	Reciprocal	Final Flood quantiles
2	0.5	297.7	356.4	226.2	293.0	302.0	355.2	356.4
5	0.8	579.3	632.4	527.4	540.2	662.2	1259.0	540.2
10	0.9	741.6	724.5	756.9	710.7	1057.9	1919.7	710.7
20	0.95	870.3	770.5	9878.0	874.3	1634.4	2370.5	874.3
25	0.96	905.8	779.7	1062.6	926.0	1873.4	2472.6	926.0
50	0.98	1000.4	798.1	1295.6	1084.2	2845.4	2690.3	1084.2
100	0.99	1075.4	807.3	1530.1	1239.6	4300.0	2806.2	1239.6
500	0.998	1194.9	814.6	2080.2	1593.2	11140.0	2902.5	2902.5
1000	0.999	1229.6	815.6	2319.7	1743.2	16769.0	2914.8	2914.8

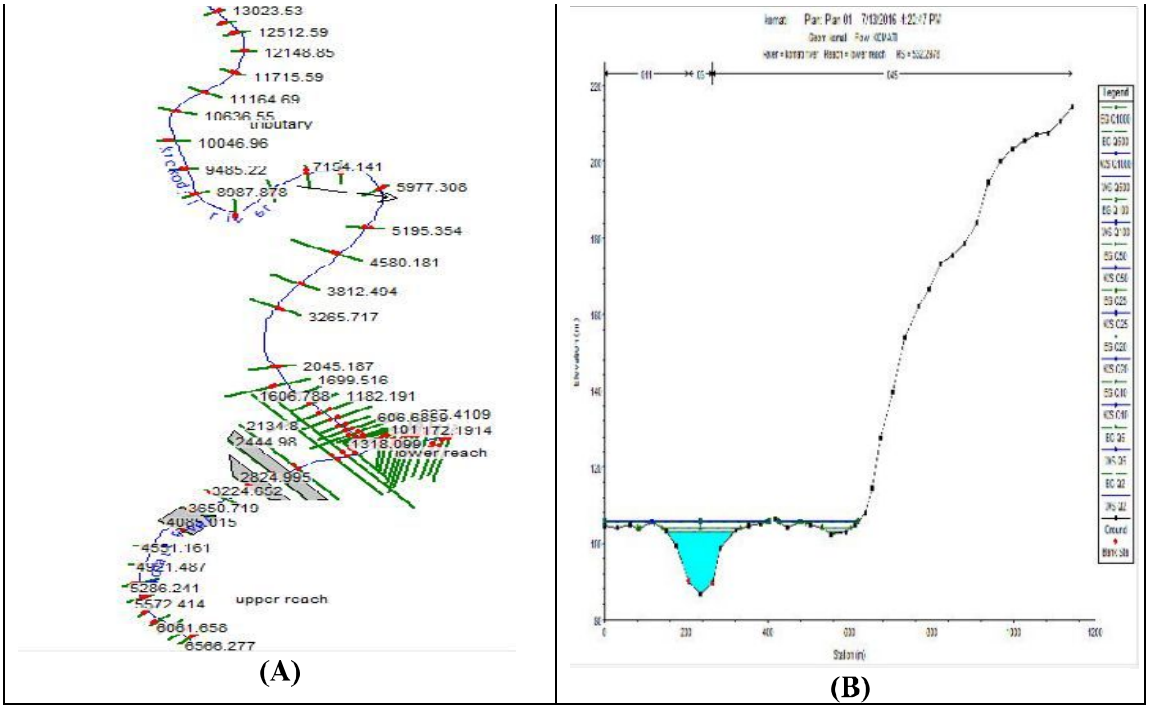

Figure 11: Extracted River Geometry for Komati and Krokodil Rivers (A) and Komati River Cross-section (B)

Flood inundation extent for different return periods

Figure 12 shows the extent of a flood inundation that is expected to recur in the study area depending on the return period. The depth of this flood ranges 10.78 m for return period of 5 years, which increases to 16.2 m for a return period 1000 years. For a 1000-year return period a flood depth of up to 16.2 m will be reached, which will inundate an approximate area of 6.18 km^2. It is evident that as flood depth increases, it is expected that more people distressed and more property will be damaged. Farmers and homesteads situated along the Komati and Krokodil rivers are the most affected by these floods. One of the areas that are likely to be affected by Komati River floods is Komati central commercial district, which is nested at the confluence of these two rivers. The other areas include

the farms and peri-urban/rural Komatipoort, while Krokodil river floods only affect peri-urban Komatipoort and the agricultural areas.

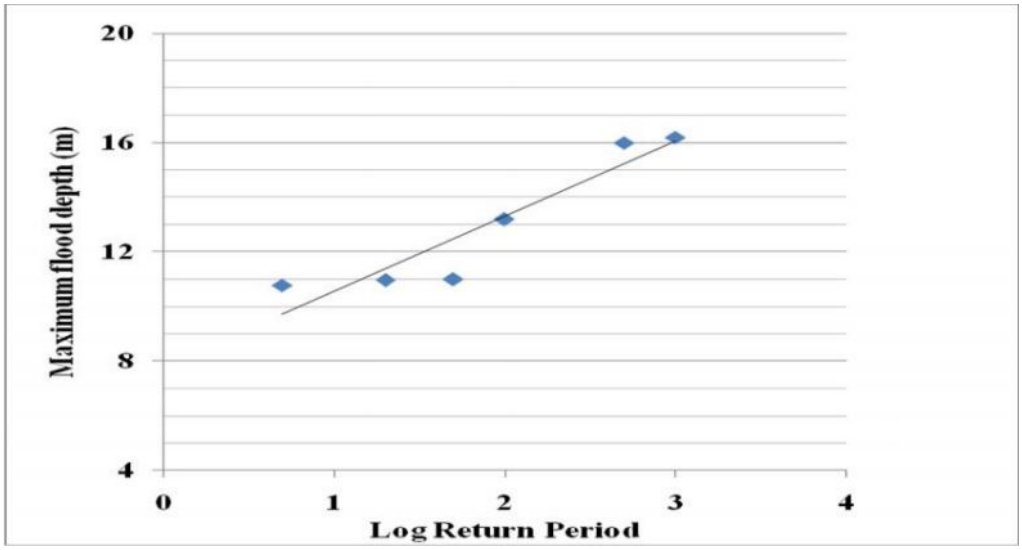

Figure 12: Flood Hazard map for various return periods

This assessment has proven to be in line with the 2014 preliminary assessment report on Mpumalanga flood incidents by The Ministry for Cooperative Governance and Traditional Affairs (CoGTA), Mpumalanga Provincial Government. According to this report, the March 2014 floods caused havoc in the Nkomazi municipality. About 553 km of municipal streets were eroded, costing the government R33.1 million (USD 2,424,872) in reconstruction costs. Five (5) Bridges were washed away, 4 Bridges were damaged and 1 Foot bridge was eroded, which required R 4.8 million (USD 351,643) to rehabilitate. About 119 houses were flooded and damaged, leading to R13.09 million (USD 958,960) in remedial costs. Farmers were severely affected as 58 water pumps were submerged in water, electric panels were damaged and 325 ha of sugarcane crops were waterlogged, bringing the total agricultural costs to an estimated R4,143,750 (USD 303,567). There were also immediate costs as people had to be airlifted since they were disconnected from other communities due to bridges that got washed away, as well as humanitarian costs in terms of temporary housing, food parcels, blankets and water for displaced families.

Flood Susceptibility Mapping

Heavy rainfall is one of the major causes of floods, hence it carries the most weight in flood susceptibility analysis. According to Figure 13(A), the northern part of Komatipoort (along Krokodil River) records the highest rainfall, while the southern part (along the Komati River) records the lowest rainfall. This makes the northern part of Komatipoort more susceptible to floods because it is situated downstream of the Krokodil River. The map also shows that 18% of Komatipoort has very low flood susceptibility, 17% has low susceptibility, 20% has moderate flood susceptibility, 24% has high susceptibility and 21% of the area has a very high flood susceptibility based on rainfall.

There are several types of land uses identified in this study area: bare soil,

urban / built-up, indigenous forest, thicket, bush land, shrub land, agricultural land (sugarcane, orchards), barren land, water bodies and wetland. According to Figure 13(B), 43% of the Komatipoort has very low to moderate susceptibility to flooding, 3% has low susceptibility, 49% is moderately susceptible, 0.5% has high susceptibility and 4.5% has very high flood susceptibility. The areas that show low susceptibility to floods are those dominated by forests and rangelands, which offers soil coverage and thus delaying flow. Komatipoort is a sugarcane area with a sugar mill, so it is hardly surprising that this area is dominated by agricultural land, which makes it moderately susceptible to floods. As much as a good portion of the Komatipoort is covered in vegetation and thus reducing its susceptibility to flooding, this town is also quite developed at the river confluence, which increases run off and thus increasing flood susceptibility. However, high susceptibility to floods was noted at the confluence of the two rivers, which is the central business district. This area is dominated by built-up spaces, which reduces infiltration and increases run-off. The map also shows high flood susceptibility along the two rivers. Since wetlands have saturated soils, they hinder infiltration, thus encouraging increased runoff, and subsequently flooding.

Mountainous areas are less likely to be scourged by floods, while flat plains and valleys are always highly susceptible to flooding. This is caused by the speed at which runoff flows on mountains, as compared to sluggish meandering in valleys, allowing for runoff accumulation and subsequently flooding. According to Figure 13(C), Komatipoort is dominantly moderately susceptible to flood susceptibility based on elevation because the area is mostly dominated by an elevation of 75 – 150 m. Komatipoort also has noticeably high susceptibility to floods, especially along The Komati and Krokodil rivers, implying that along the rivers, the area has a low elevation. The map also shows that only 0.6% of Komatipoort has high flood susceptibility, 83% of this area is moderately susceptible, 16% has low susceptibility and 0.4% has very low flood susceptibility based on elevation. According to Figure 13(D), Komatipoort is dominantly highly susceptible to flood based on slope. About 37% of Komatipoort area has very high susceptibility to flooding based on slope (slope range of 0 – 7%), 32% of Komatipoort has high susceptibility (slope range of 8 – 14%), 20% has moderate susceptibility (slope range of 15 – 21%), 9% has low susceptibility (slope range of 22 – 28%) and only 2% of this area has very low susceptibility (slope range of 29 – 35%).

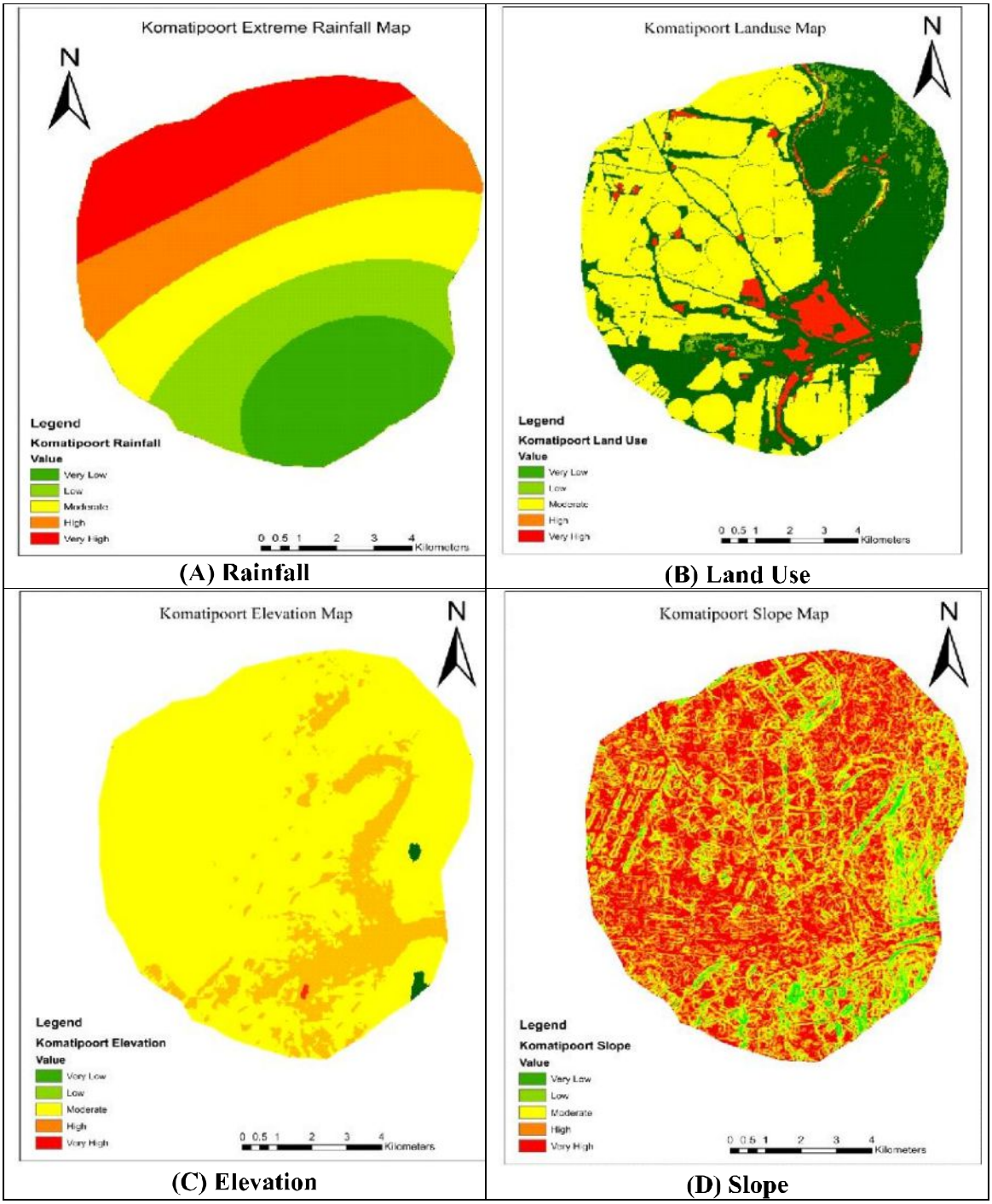

Figure 13: Komatipoort flood susceptibility maps based on various indicators.

Figure 14(A) shows that Komatipoort has very high susceptibility to floods based on drainage density. High drainage density increases the risk associated with floods. It was observed that 33% of Komatipoort has very high flood susceptibility based on drainage density, 25% has high flood susceptibility, 13% of the area is moderately susceptible, 21% has low susceptibility, but only 2% of the area has very low flood susceptibility. Road is one of the important anthropogenic factors inducing flood hazard, because they disturb the free flow of water. The porosity

of soil is traded with impervious surfaces such as tar that accumulate little water, reduce permeation of water into the ground and hasten runoff, subsequently increasing susceptibility to flooding. Higher road density increases susceptibility to flooding. The road density map of Komatipoort was derived from a roads map through Focal Statistics in Arc GIS. Figure 14(B) shows that Komatipoort has dominantly very high flood susceptibility based on road density. About 69% of Komatipoort has very high flood susceptibility based on road density, 18% of the area has high flood susceptibility, 6% of the area has moderate flood susceptibility, 5% has low susceptibility and only 3% of the area has very low flood susceptibility based on road density. The conclusion drawn here is that urban built up areas, which are hugely characterized by impervious surfaces and limited vegetation, are prime victims for flood (Liyanarachchi, 2004; Lawal *et al.*, 2014).

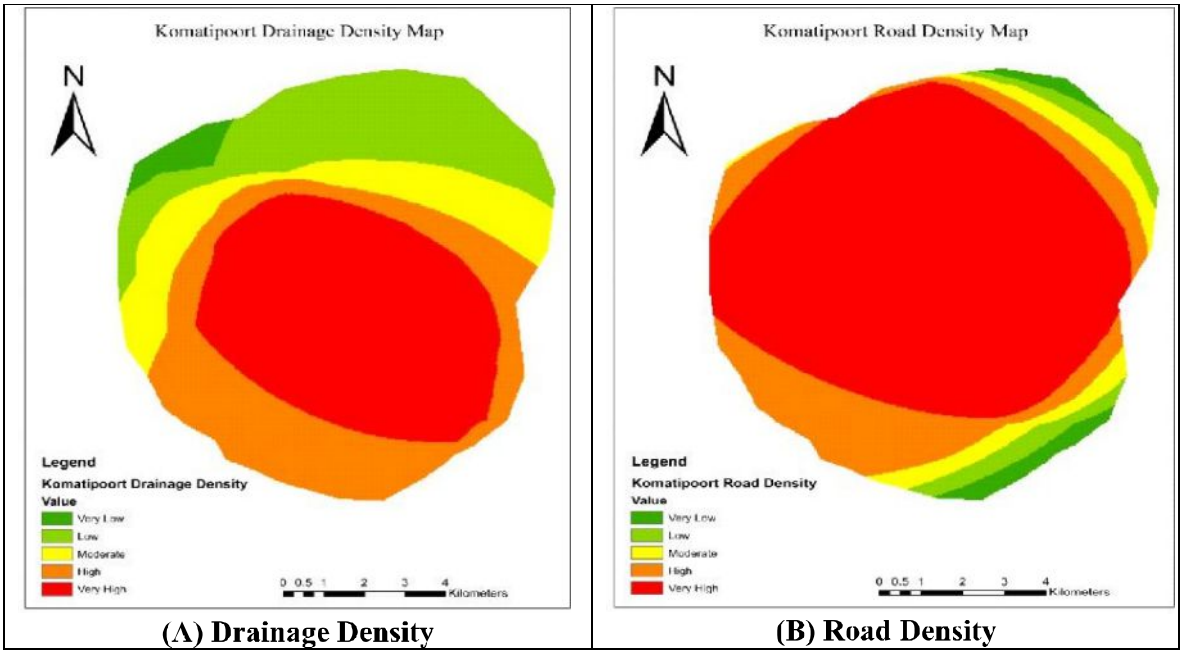

(A) Drainage Density **(B) Road Density**

Figure 14: Komatipoort flood susceptibility map based on (A) Drainage density and (B) Road density

Figure 15 shows Komatipoort has a has a dominantly high susceptibility to flooding particularly where there are high rainfalls, high road density, high drainage density, low elevation, low slope and when the land use is dominantly urban built-up, wetlands and water bodies. About 18% of Komatipoort has very high susceptibility to flooding, 17% has high susceptibility, 20% is moderately susceptible, 24% has low susceptibility and 21% has a very low susceptibility to flooding.

The accuracy of results presented here are a function of availability and accuracy of the data. As pointed out by Els (2011), data availability for the Republic if South Africa is restricted, especially for small towns. A 30x30 m resolution Digital Elevation Model (DEM) with was utilized for this study, which is a low resolution DEM and it proved to be insufficient for hydraulic modeling of river channels because it could not capture and represent sharp changes in the topography of the terrain. A DEM with a high resolution (<10 m) would have been more suitable,

ideally used in concurrence with a topographic map for clear display of structural features. For this study, a land use map used in conjunction with a geo-referenced Google earth map proved to be a useful tool in identifying the flooded areas in the absence of a topographic map of the area. Lack of long continuous flow data is another issue for the study area. Only one gauging station has data ranging from 1960 to 2016, the other stations have much shorter data series, which raised the need to extend this data through hydrological analysis.

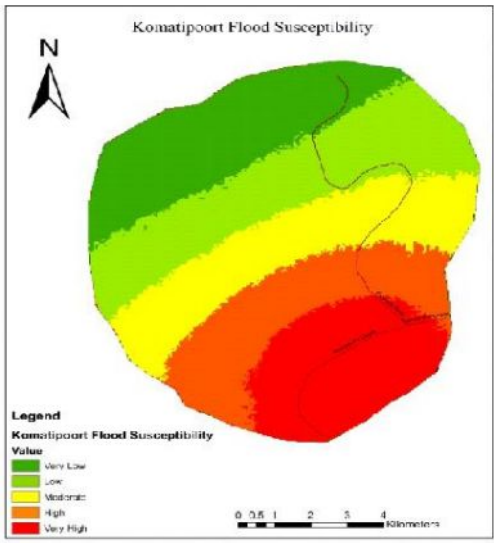

Figure 15: Komatipoort flood susceptibility map

CONCLUSIONS

In conclusion it was observed that the best probability distributions for Krokodil River flow data was the Log Logistic (3P) for discharges that are less or equal to 400 m^3/s, Reciprocal for discharges at varies between 400 to 500 m^3/s and Gamma for discharges ranging above 500 to 1200 m^3/s. The extent of a flood inundation that is expected to recur in the study area was dependent on the return period. The depth of this flood ranges 10.8 m for return period of 5 years to 16.2 m for a return period 1000 years, which covers an approximate area of 6.2 km^2. It can be concluded that there is indeed a flood problem along the Komati and Krokodil rivers in Komatipoort. This flood affects the farms and homesteads along the banks of these rivers, the urban residential area, the central business district as well as the grasslands and natural forests. The results also show that the area is generally susceptible to floods due to a combination of anthropogenic factors (Land use and road density), hydrological factors (drainage density), geomorphological factors (slope and elevation) as well as meteorological factors (rainfall). Flood frequency analysis showed the maximum flow of 1163 m^3/s for a return period of 1000 years for Krokodil River and a maximum flow of 2915 m^3/s for the same return period for Komati River. The results also showed that a flood of 1066 m^3/s is likely to occur every 50 years, which has proven to be accurate considering that in the flow data for Krokodil River observed over 55 years, the maximum flow recorded is 1169 m^3/s, and the second highest flow is 1022 m^3/s.

ACKNOWLEDGEMENT

This paper presents part of the research study of Masters of Integrated Water Resources management dissertation by the first author, which was pursued at the University of Dar es Salaam under a WaterNet fellowship. The authors wish to express their gratitude to WaterNet for the financial support extended to the first author.

REFERENCES

Balica S., Douben N. and Wright N.G. (2009). Flood vulnerability indices at varying spatial scales article in water science and technology. Available online at http://www.researchgate.net/publication/38099496. Retrieved on 27th November 2015.

Bishaw K. (2012). Application of GIS and Remote Sensing Techniques for Flood Hazard and Risk Assessment: The Case of Dugeda Bora Woreda of Oromiya Regional State, Ethiopia, Ethiopian Civil Service University. Addis Ababa, Ethiopia. Paper for the Berlin Conference on the Human Dimensions of Global Environmental Change.

Department of Cooperative Governance and Traditional Affairs (CoGTA) (2014). Preliminary Report, Cooperative Governance Traditional Affairs, Pretoria, Republic of South Africa.

Daniell T. (2014). Hydrology in a Changing World: Environmental and Human Dimensions, International Association of Hydrological Sciences, IAHS, 36.

Els Z. (2011). Data Availability and Requirements for Flood Hazard Mapping in South Africa, Stellenbosch University. Available online at http://scholar.sun.ac.za. Retrieved on 9th June 2018.

IFRC (2015). Analysis of legislation related to disaster risk reduction in South Africa, International Federation of Red Cross and Red Crescent Societies, Geneva, Available online at http://www.ifrc.org/idrl.17 - 20. Retrieved 04th December 2017.

Khumalo N. (2016). Modeling of Flood Hazard and Susceptibility in Komatipoort Area in South Africa. Master of Integrated Water Resources Management Dissertation, Department of Water Resources Engineering, University of Dar es Salaam, Tanzania.

Kumpulainen S. (2006). Vulnerability Concepts in Hazard and Risk Assessment, Natural and Technological Hazards and Risks Affecting the Spatial Development for European Regions, Geological Survey of Finland, Special paper 42: 69 - 74.

Kundzewics Z.W. (2012). Changes In Flood Risk in Europe, Institute of Agriculture and Forest Environment, Polish Academy of Sciences, Poznan, Poland, IAHS and CRC press, 13 – 22.

Kundzewicz Z.W., Kanae S., Seneviratne S.I., Handmer J., Nicholls N., Peduzzi P., Mechler R., Bouweri L.M. , Arnell N., Mach K., Muir-Wood R., Brakenridge R., Kron W., Benito G., Honda Y., Takahashi K. and Sherstyukov B. (2012). *Flood risk and climate change: global and regional perspectives*. Hydrological Sciences Journal, 59(1): 4 – 6.

Lawal D.U., Matori A.N., Yusuf K. W., Hashim A.M. and Balogun A.L. (2014). Analysis of flood extent extraction model and the natural influencing factors: A GIS-based and remote sensing analysis, Civil Engineering Department, University of Technology PETRONAS.

Liyanarachchi P. (2004). Application of Geographical information systems for flood risk mapping, University of Ruhuna, 104.

Malczewski J. (1999). GIS and Multicriteria Decision Analysis, New York: John Wiley and Sons.

Musungu K., Motala S. and Smit J. (2012). Using Multi-criteria Evaluation and GIS for *Flood Risk Analysis in Informal Settlements of Cape Town: The Case of Graveyard Pond*, Geomatics Division, University of Cape Town, Cape Town, South Africa, Civil Engineering and Surveying, Cape Peninsula University of Technology, Cape Town, South Africa, South African Journal of Geomatics, 1(1): 14 - 19.

Sayers P., Li Y., G. Galloway, Penning-Rowsell E., Shen, F. Wen K., Chen Y., and Le Quesne T. (2013). Flood Risk Management: A Strategic Approach. Paris, UNESCO. 30 – 38 http://www.adb.org/. Retrieved on 04th December 2015.

Schanze J., Zeman E. and Marsalek J. (2006). Flood Risk Management: Hazards, Vulnerability and Mitigation Measures, Springer, 149 – 167.

Sredojevic D., and Simonovic S. (2009). Water Resources Research Report, City of London: Vulnerability of Infrastructure to Climate Change, Background Report 2 - Hydraulic Modeling and Floodplain Mapping, The University of Western Ontario Department Of Civil and Environmental Engineering, Report No: 069, September 2009, retrieved 01 June 2016.

Swades P. and Surajit L. (2012). *Flood Intensity And Potential Flood Loss Estimation In Dwarka River Basin Of Eastern India*, Department of Geography, University of Gour Banga, Malda, West Bengal, India, International Journal of Geology, Earth and Environmental Sciences, 2(1): 116-122. Available online at http://www.cibtech.org/jgee.htm,.

Yashon O., Ouma 1. and Tateishi R. (2014). Urban flood vulnerability and risk mapping using Integrated Multi-Parametric AHP and GIS: Methodological overview and case study assessment, Department of Civil and Structural Engineering, Moi University, Centre for Environmental Remote Sensing (CEReS), Chiba University. Available online at www.mdpi.com/journal/water.